Influence of small gaps in AC magnetic field shielding for image quality of MRI devices

Rafael Navet de Souza
FSE in MRI / Department of Biomedical Engineering
Siemens Healthineers Brazil/ University of Campinas
Rio de Janeiro, Brazil
navet_r@yahoo.com.br

Sergio Santos Muhlen
Department and Center of Biomedical Engineering
University of Campinas
Campinas, Brazil
smuhlen@unicamp.br

***Abstract*—Magnetic Resonance Imaging (MRI) is a technique that produces high-resolution volumetric images of the body without using ionizing radiations. The quality of images is greatly disturbed by environmental magnetic fields, especially of 50/60 Hz, and particularly on MRI equipment with permanent magnets, which results in the need of shielding the room where the equipment is installed. This study was carried out to quantify the influence of small gaps on the shielding junctions in the image quality of MRI equipment with permanent magnets. We present the influence of gaps in the shielding effectiveness (SE) for alternating current (AC) magnetic fields in MRI exam rooms for both ferromagnetic (NGO Fe-Si alloy) and conductive (Al) shielding and compare them. We have created a computational model of the shielding and compared the simulations results with experimental measurements using a metallic box with dimension of 1m³ and gaps of 0.5 mm in the sheets junctions. The aluminum shield has proved to be advantageous for AC magnetic field shielding but suffers greater influence in the SE when the gaps are taken to account.**

Keywords—Magnetic shielding; Hospital environment; Magnetic resonance

I. INTRODUCTION

Magnetic Resonance Imaging (MRI) equipment uses magnetic fields and radiofrequency (RF) waves. The technique is based on the phenomenon of nuclear magnetic resonance (NMR), discovered in 1938 and used since then for the analysis of chemical compounds. NMR is a physical phenomenon in which the nucleus of an atom of a given substance absorbs and emits energy in the form of RF in the presence of an external magnetic field. It is possible to determine properties of the substance by correlating the energy absorbed at each frequency of the magnetic spectrum (in the MHz range), such as spectroscopy [1].

The magnetic fields generated by the equipment make the protons of hydrogen atoms (commonly used in commercial equipment) of the water molecules present in the human body to align (similarly to a compass needle when placed next to a magnet). When an RF pulse is generated and radiates the body, some of these protons absorb the RF energy and change its direction. The fields of the individual nuclear magnets can be summed to create a resulting magnetic field, which induces current in a receiving coil or antenna. When the RF pulse ceases, the protons return to their original position (aligned with the static magnetic field of the equipment), releasing the absorbed energy and inducing electric current in the antenna (or coil) in the form of an exponential damped pulse. This very thin signal is captured, processed and sent to a computer system for reconstruction of the anatomical image.

Excitation as well as spatial encoding uses the linear relation of Larmor frequency and magnetic field strength. In order to have the magnetic field strength as a function of location, a magnetic field gradient is superimposed during excitation and during data acquisition for the purpose of spatial encoding in x, y and z direction. The Larmor frequency is represented by:

$$\omega = \gamma \boldsymbol{B_0} \tag{1}$$

where: ω is the Larmor frequency (MHz), γ is the gyromagnetic ratio (MHz/T) and B_0 represent the magnetic field strength (T).

Currently, there are two types of MR scanners: superconductive and permanent magnets. Permanent magnets are more susceptible to external interference mainly because of their magnet simplicity and the absence of an active compensation system to external interferences integrated with the equipment.

When MRI equipment is installed in hospital environment, a magnetic shielding is often required to avoid uncontrolled exposure of the surrounding environment to the strong magnet field dispersion and also to reduce the influence of the local magnetic fields on the field homogeneity of the equipment [2]. This shielding is generally constructed using ferromagnetic materials or good conductive metals such as aluminum or copper. The preferred ferromagnetic material is Fe-Si non-grain-oriented (NGO) alloy, but the non-linearity of its magnetic properties must be considered in the design [3].

For MRI scanners, a reduction in the effectiveness of the shielding may result in image artifacts from parasitic currents induced in the protection or any conductive part of the MRI apparatus. If the AC magnetic fields are not mitigated as required in the design, the resulting magnetic field within the shield will influence the gradient field, mainly for spin echo sequences where the echo time (TE) can be adjusted as TE = 20 ms. Eddy currents generate field gradients that match with the image gradient pulses such as that the real gradients experienced by spins on image objects are not exactly the same as those that were programmed to produce and rebuild

CNPq Brazil and Siemens Healthineers Brazil sponsored this study.

the image. Therefore, this error in local gradients (which are not taken into account in the reconstruction software) produces geometric distortion in the final images [4]. Figures 1 and 2 show some examples of gaps normally found in shielding for MRI systems.

Fig. 1. Shielding with bad connections between plates joints, creating unwanted gaps (white arrows).

Fig. 2. Gap caused intentionally by the shield installer (white arrow).

MRI uses as default frequency-encoding and phase-encoding that are essential to MR image creation [5]. Unwanted gaps in the shielding can produce phase errors that can arise from minor deviations in the linear course of the gradient. The mismatch in phase causes the appearance of "ghosts" on the reconstructed images. For example, on images acquired with a single-shot echo-planar imaging sequence, the "ghost" appears as an additional image with reduced intensity that is shifted by half of the field view, as shown in Figure 3. This type of "ghost" artifact is commonly referred to as an N/2 ghost [6].

There are two kinds of shielding for alternating current (AC) magnetic fields: passive and active. Passive shielding are easy to construct, cheaper and are normally used to reduce the external AC magnetic field levels on MRI exam rooms. The passive shield is assembled applying ferromagnetic or conductive plates in the wall.

Active shield consist in the use of software or coils mounted inside the room to compensate the external magnetic field. For MRI equipment with permanent magnets a hybrid shielding (passive and active shielding) is generally used due to the high sensibility to external magnetic field. Depending on the manufacturer the shielding can be installed using modular plates or plates fixed on the room walls.

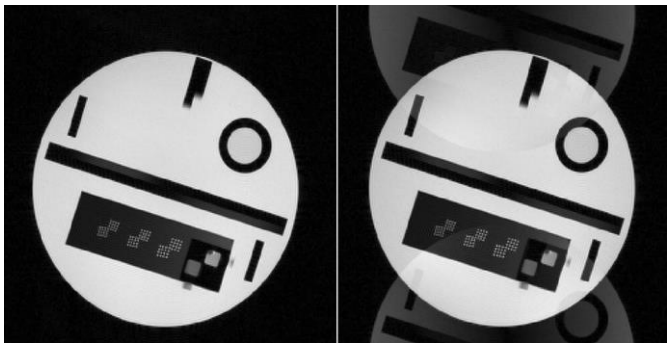

(a) **(b)**

Fig. 3. Effect of phase errors at MR imaging in a phantom. **(a)** Initial image, acquired by using a fast spin echo sequence, without ghost artifacts. **(b)** Image acquired with single-shot echo-planar imaging shows an N/2 ghost, a typical result of phase error.

The objective of this study is to evaluate the influence of small gaps in AC magnetic field shielding which can affect directly or indirectly the quality of images on MRI devices. This study is motivated by the high demand for installation of MRI equipment in Brazil and the diversity of techniques to execute the shielding (assembling and deployment) among the many manufacturers. Although the effect of gaps in magnetic shielding is not a new event for other applications, we performed experiments and computational simulations using ferromagnetic and conductive materials to compare the influence of these gaps in the Shielding Effectiveness (SE).

II. MATERIALS AND METHODS

The experiments and computational simulation were performed using ferromagnetic and conductive materials for shielding AC magnetic fields. In our experiments we used the "Aluminum alloy 1200" as conductive material and "Fe-Si alloy E185 NGO" (non-grain-oriented) as ferromagnetic material. These alloys are commonly used on shielding of MRI exam rooms because of their affordability and availability in Brazil and are also similar to the materials commonly used to MRI room shielding in Japan.

A. Experiments

The experiments aimed to compare the influence of gaps in the SE of the Al and Fe-Si NGO shields in a controlled environment. The experiments consisted in performing measurements on the intensity of 60 Hz magnetic field by varying the distance between the measuring point and the source, the thickness and the material of the shielding. The shield structure is a metallic cubic frame (1 m^3) in which the plates of shielding materials (Al or Fe-Si NGO) are fastened, so as to make it easier to change the number of plates (total thickness) and types of materials. The shielding joints on the cube edges were maintained open to create a small gap. Figure 4 shows the prototype with the gaps in the plate edges.

Measurements of shielding efficiency were performed using a triaxial magnetic field sensor (magnetometer) (STL, model DM-050) mounted on a tripod inside the cubic shield and connected to a computer via a coaxial cable. The density of magnetic flux $\vec{B}$ obtained by the magnetometer was expressed in nanotesla [nT].

The 60 Hz magnetic field was generated by a coil of a single rectangular turn (19 m × 12 m loop), implemented with a flexible cable (ϕ 4 mm^2) suspended 60 cm from the ground. This cable supplied a resistive load (2 heaters) to produce a current of 18.4 A_{rms}. Figure 5 shows the electrical circuit used on the computational and experimental setup. The measuring points P1-P5 were varying from 1 to 5 m from magnetic field source in steps of 1 m.

Fig. 4. Cubic structure (1×1×1 m) covered with metallic plates with small gaps in the edge joints used on the experiments (between white arrows).

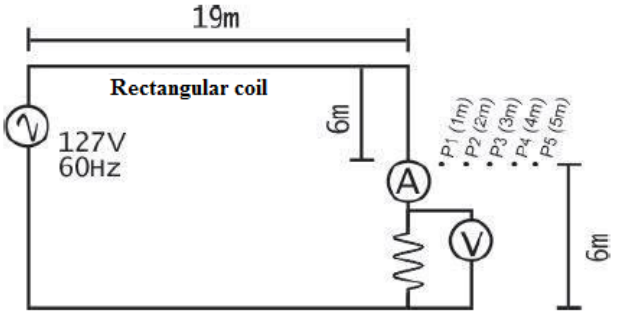

Fig. 5. Circuit used for computational simulation and experiments design. A rectangular loop conductor was used to generate the magnetic field, and the points P1-P5 are the measuring points representing the position in the center of the shield.

B. Computational simulation

Computational simulation was performed with the package Comsol Multiphysics® [7], for a setup with a wire conducting a known current, and a cubic metallic box with a small gap of 0.5 mm of thickness in all plate's edges, as performed on the experiments. Arrows in Figure 6 show the gaps representing imperfections in the joints of the metal plates.

In addition to the simulations considering the imperfections in the shield, more simulations were also performed considering a perfect shield, without gaps in the joints. Due the low density of magnetic flux [nT], we did not consider the non-linearities of Fe-Si NGO, assuming that the relative permeability was constant. The parameters used on the simulations are shown in Table I and the material properties are shown in Table II.

III. RESULTS

The result graphics are separated in order to facilitate the understanding. The results showed in Figure 7 represent the SE [dB] for aluminum with gap obtained both from the computational simulation and experiments. Figure 8 represents the results of SE obtained by computational simulation for aluminum shielding with and without gap.

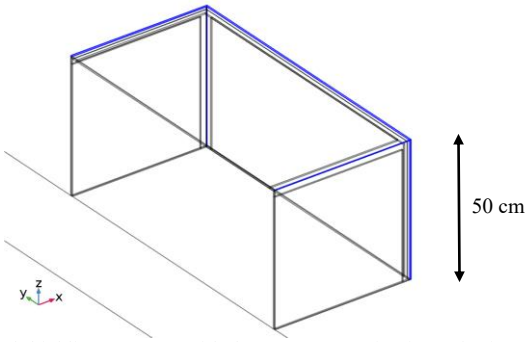

Fig. 6. 1/4 of shielding structure with the gap representing imperfections in the joints of the metal plates.

Results for Fe-SI NGO are showed in the Figures 9 and Figure 10. Figure 9 represents the shielding effectiveness for Fe-SI NGO with gap obtained in the computational simulation and experiments, and Figure 10 represents the results obtained by computational simulation for Fe-Si NGO shielding with and without gap.

TABLE I. Parameters used for simulation.

Description	Value
Frequency f	60 Hz
Temperature T	20 ºC
Current I	18.4 A_{rms}
Thickness t	0.5 to 3 mm
Distance d	1 to 5 m

TABLE II. Material properties.

Material	Electrical conductivity [10^6 S/m]	Relative permeability [H/m] @1.5T
Aluminum	34.5	1
Fe-Si NGO	2.6	1530

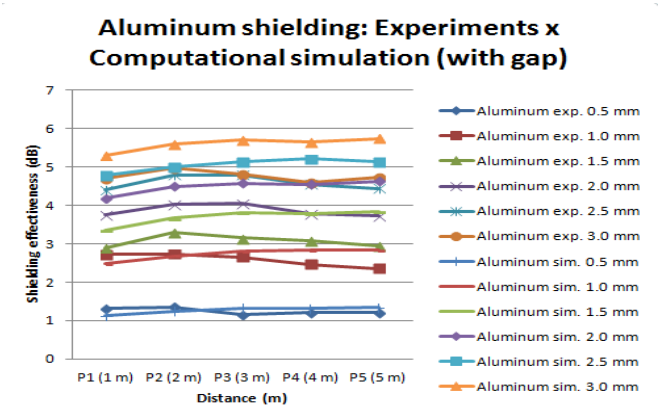

Fig. 7. Results obtained by computational simulation (sim.) and experiments (exp.) for shielding effectiveness using Aluminum shielding with different thicknesses.

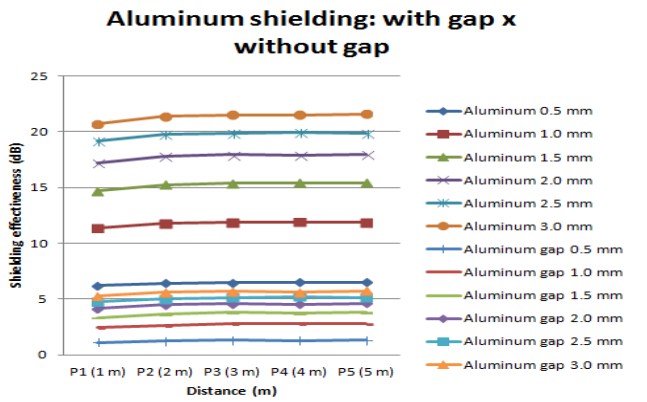

Fig. 8. Results obtained by computational simulation for shielding effectiveness using Aluminum shielding with different thicknesses and gaps.

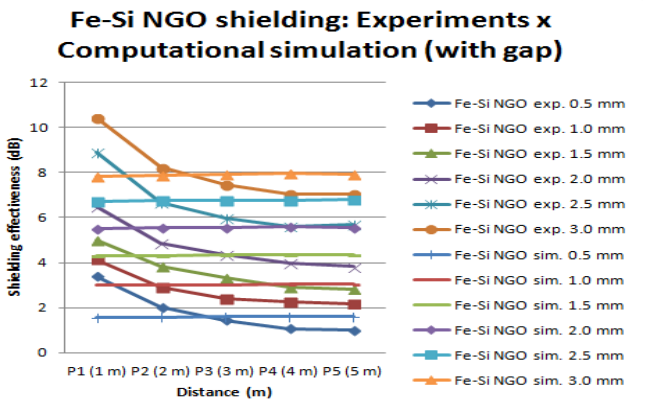

Fig. 9. Results obtained by computational simulation (sim.) and experiments (exp.) for shielding effectiveness using Fe-Si NGO shielding with different thicknesses.

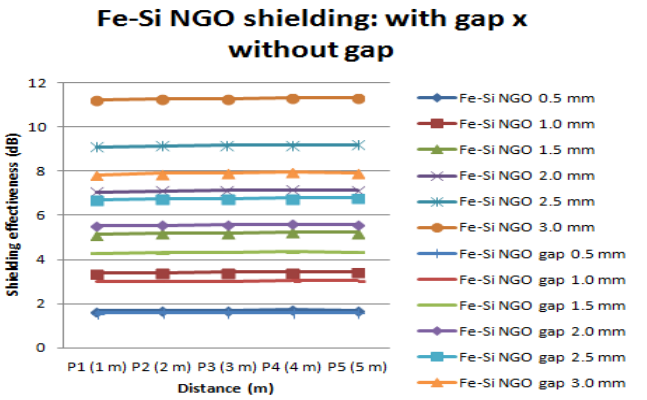

Fig. 10. Results obtained by computational simulation for shielding effectiveness using Fe-Si NGO shielding with different thicknesses and gaps.

IV. Discussion

The results in Figure 8 reveal that the gap in the aluminum shielding caused a reduction in the shielding effectiveness of 5 to 15 dB depending on the shielding thickness. Figure 10 shows that the influence of gaps in the Fe-Si NGO shielding caused a decrease of 1 to 5 dB on the SE, depending of the shielding thickness.

The results of computational simulation for Fe-Si NGO doesn't show the decrease of SE as the distance increase because we did not consider the non-linearities of Fe-Si NGO, as mentioned above, assuming that the relative permeability was constant. This explains the differences between computational simulation and experimental results.

It is well known that aluminum is more effective than Fe-Si NGO for AC magnetic field shielding but when gaps in the shielding installation are considered, its shielding effectiveness can be considerably reduced to be less effective than shielding using ferromagnetic materials, as shown in Figures 8 and 10. On the other hand, shield joints are easier to construct using conductive materials, usually easier to bend, weld or rivet, and to maintain, since they do not rust.

The most common gap created in shielding installation occurs in the shielding joints as shown in the Figure 1. Other types of gaps can occur when the shield installer leaves small gaps purposive due to the difficulty to cut the plates according the project design, thinking that this small gap will not cause problems for image quality of the equipment as shown in the Figure 2.

V. Conclusions

The results indicate that the influence of gaps in the shielding of the AC magnetic field may impair magnetic resonance imaging due to artifacts in the image, especially for MRI equipment with permanent magnets, which are more susceptible to AC magnetic field interference. These devices have as requisite for installation a maximum AC magnetic field in the order of hundreds of nT.

After experiments and computational simulation, it was possible prove that a small gap can cause a big influence in the shielding effectiveness. However, if the shielding manufacturer consider precisely all joints in the shield project the chances of undesirable gap occur can be reduced.

VI. References

[1] R.N. Souza and S.S. Muhlen, "Advantages in the application of conductive shielding for AC magnetic field in MRI exam rooms", World Congress on Medical Physics andd Biomedical Engineering 2018. IFMBE Proceedings, vol. 68/3, pp. 577-580, May 2018.

[2] S. Noguchi and A. Ishiyama, "Optimal design method for MRI superconducting magnets with ferromagnetic shield" IEEE Transaction on Magnetics, v. 29, n. 2, pp. 1240-1244, 1993.

[3] K. Yoshizawa, S. Noguchi and H. Igarashi, "Influence of magnetic property of ferromagnetic shield on high field magnet analysis," IEEE Transaction on Applied Superconducivity, v. 21, n. 3, pp. 2088-2091, 2011.

[4] L. J. Erasmus, D, Hurter, M. Naudé, H.G. Kritzinger and S. Acho, "A short overview of MRI artefacts," SA Journal of Radiology, August, 2004.

[5] P. Reimer, P.M. Parizel, J.F.M. Meaney and F.A. Stichnoth, Clinical MR Imaging: A Practical Approach, 3 rd ed. New York: Springer, 2010.

[6] J. Zhuo and R.P. Gullapalli, "AAPM/RSNA physics tutorial for residents: MR artifacts, safety and quality control," Radiographics, v. 26, n. 1, pp. 275-297, 2006.

[7] www.comsol.com